SCHLIEREN IMAGING OF NARROW CHANNEL COMBUSTION

T.R. Ritchie, B.Z. Dlugogorski, M.A. Delichatsios, B. Moghtaderi and E.M. Kennedy
Process Safety and Environment Protection Research Group
School of Engineering, Faculty of Engineering and Built Environment
The University of Newcastle, Callaghan, NSW 2308, Australia

ABSTRACT

Schlieren imaging was trialled as a technique for investigating thermal properties of a flame in a narrow channel apparatus. The method was used in conjunction with direct photography to gain knowledge of heat transfer in the flame and the profile of the flame front. Quantities including cross-sectional flame shape, gaseous thermal length and solid thermal length were able to be measured. The experiment was carried out for floor and ceiling spread in a horizontal chamber at two different channel heights (6.5 and 4 mm), and for low and high flow rates of pure oxygen (4.5 and 16.5 cm/s respectively). It was found that the combustion conditions did not successfully approximate a microgravity environment for the 6.5 mm channel at low gas flow rates, with floor and ceiling spread flames differing significantly. This is believed to be due to poor transport of hot fuel vapour away from the fuel surface. These effects were reduced in the 4-mm channel and at higher flow rates.

KEYWORDS: Flame spread, Schlieren, Narrow channel, Microgravity, Solid fuel

INTRODUCTION

The narrow channel apparatus (NCA) is a device designed to study the combustion of solids under simplified conditions. It consists of an enclosed channel with such a narrow vertical dimension as to effectively eliminate buoyancy effects and convective transport of mass and heat. A thermally thick solid fuel lining the channel is ignited at one end, and the flame propagates at a steady rate into an opposed flow of oxidiser, which is introduced via a diffuser at the opposite end of the fuel. Flow is laminar and two-dimensional. Due to the reduction of buoyancy effects, the NCA can be considered to mimic a microgravity environment for flame. [1] These simplified conditions for combustion have led to the apparatus being useful for studying fire safety in spacecraft, for testing of solid materials flammability or fire suppressant effectiveness [2], and for research into the fundamental mechanisms of flame propagation.

The basic mechanism of creeping flame spread is shown in Fig. 1. The heat of the flame pyrolyses the fuel, which forms a vapour. The flame front occurs at the region where the fuel vapour and oxidiser mix in stoichiometric ratio. Some of the released energy is transferred to the unburnt fuel bed, thus completing the energy cycle necessary to maintain the fire-spread process. A close-up of the flame tip is shown in Fig. 1b with solid and gaseous thermal lengths L_s and L_g marked in both the vertical and horizontal directions. If gas-phase conduction is the driving force, L_{gx} and L_{sx} will be approximately equal.

The rate of spread is determined by how fast the flame heats the solid fuel from ambient temperature T_∞ to vapourisation temperature T_v. Heat transfer is dominated by solid-phase conduction. It has been suggested, however, that in true microgravity, the gas-phase conduction will dominate near the quenching regime. [4] Gas-phase radiation has also been shown to play a significant role in microgravity flame spread. [5] Flame spread rate has been found to increase as gas velocity and oxygen concentration are increased. The flame length increases significantly with an increase in the gas velocity, but does not have a statistically significant dependence on the oxygen concentration. [2]

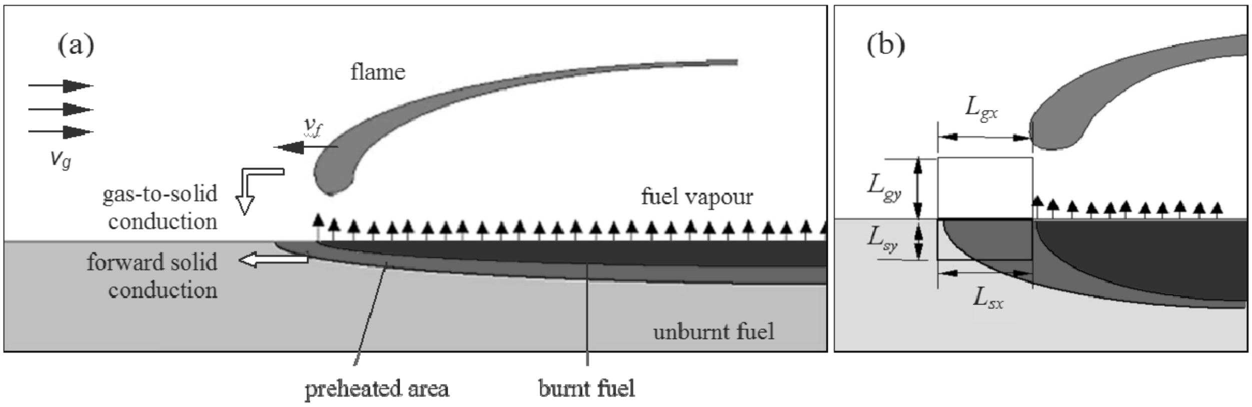

FIGURE 1. (a) Basic mechanism of creeping flame spread (b) Flame tip with thermal lengths (Image adapted from Bhattacharjee [3])

Delichatsios et al. [2] equate expressions for the convective energy Q_c needed to heat the solid fuel to its ignition temperature, and the energy E given by the flame near the front, to derive an energy balance relationship that predicts a proportional relationship between oxygen concentration and the quantity $H^{1/4}$ $v_g^{-1/4}$ $v_f^{1/2}$, for a channel height H, gas velocity v_g and flame speed v_f . This was observed experimentally. Used in the derivation are expressions for L_{gx}, given by:

$$L_{gx} = \sqrt{\alpha_g \frac{H}{v_g}} \qquad [1]$$

where α_s ($=k/\rho C_p$) is the thermal diffusivity of the solid, and an expression for flame length as a function of gas velocity and chamber height is given by:

$$L_f \propto \frac{v_g H^2}{\nu_g} \qquad [2]$$

where ν_g is the gaseous kinematic viscosity.

Visualisation of the cross-sectional flame profile can help determine how to model gas flow, as the boundary layer shape determines the gaseous diffusion length scale L_{gx}, which in turn controls the gas-phase conductive heat transfer from the flame to the solid. This is crucial to carrying out the energy balance.[6] It has also shown that the structure of the flame leading edge determines the flame spread rate. [5]

Previous methods of gaining information about flame profiles include particle tracking techniques such as particle imaging velocimetry[7], thermal imaging techniques including thermocouple measurements and infrared thermography[7-9], and optical imaging techniques such as direct photography[10] and interferometry[7]. For obtaining thermal flame-profile information in an NCA, the non-invasive optical imaging techniques are the most useful. Thermal imaging techniques are complicated by viewing through glass windows in contact with the flame, and thermocouples have been shown to be impractical at the scales required to measure the flame without interfering with the flow.[11] In the current work, direct photography and schlieren imaging were employed.

Schlieren refers to a class of optical techniques for visualising refractive index changes in transparent media. It was originally used in Germany for the detection of inhomogeneous regions in optical glass which were often in the form of streaks (or Schliere, in German) and is nowadays used extensively in aerodynamic research for studying high-speed airflow. It has found increasing use in combustion research in recent years.[12,13] The technique relies on the fact that temperature changes in a gas cause changes in density, which in turn effect refractive index changes. These cause light rays passing through a test area to be deflected according to the encountered gradient of index, and hence of temperature. A filter then selectively blocks light of certain deflections, resulting in an image in which temperature changes are visible as variations in light intensity.

A typical schlieren arrangement is depicted in Fig. 2. A collimated light source illuminates the test area. A focusing lens placed on the other side of the test chamber focuses the light at point F. A second focusing lens re-collimates the beam for projection onto a viewing screen. A knife edge is located in the focal plane of F, and is carefully adjusted to just intercept the undeflected rays at F. Once this is achieved, undeflected light is prevented from reaching the screen.

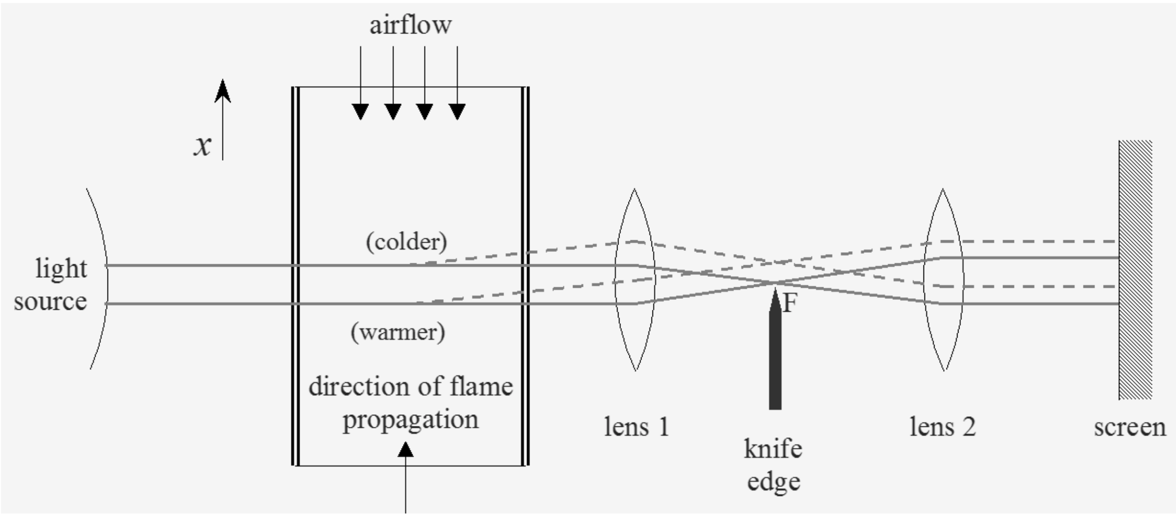

FIGURE 2. A schlieren arrangement involving the NCA (top view). A simple, arbitrary temperature profile has been illustrated. Undisturbed rays are shown in full, disturbed rays shown dotted.

If a temperature gradient is present in a direction perpendicular to the knife edge, a deflection of the light rays will occur. This will cause the rays to focus at a different point in the focal plane, thus either avoiding the knife edge (for a positive gradient, as diagrammed) or being obscured by the knife edge (for a negative gradient). Thus, thermal gradients become visible on the screen as areas of high or low intensity. Thermal gradients parallel to the knife edge (i.e. in the vertical direction) will not be visible using the setup in Fig. 2. To view these gradients, the knife may be repositioned in the horizontal direction, or two perpendicular knives in an L-configuration may be used. Circular graded filters, transparent in the centre and darkening radially to black (or passing through a colour spectrum), have also been used to obtain greyscale (or coloured) schlieren images.[14]

In the current work, schlieren and direct photography were used to study the flame profile for two oxidiser rates and two channel heights for the NCA. The results were compared to proposed models of flame spread.

EXPERIMENTAL METHOD

A schematic of the experimental setup is shown in Fig. 3a. Pure oxygen is introduced into the NCA at a rate controlled by a mass flow controller. A gas diffuser at the inlet of the NCA distributes the gas uniformly across the channel cross-sectional area.

Clear PMMA was chosen as the fuel due to its well-documented thermal properties. The fuel sheets are 10 mm thick, 360 mm long and 112 mm wide. As depicted in Fig. 3b, two pyrex glass spacers are placed lengthways along the walls of the chamber, and a pyrex glass ceiling plate is placed on top. The height of the chamber is thus determined by the height of the spacers. The ceiling plate is marked with horizontal lines at 10 mm intervals, providing a reference for measuring rate of flame spread. Two pairs of 60 mm wide gaps in the sides of the chamber allow side viewing of the flame. For direct photography, the modified spacer/window arrangement shown in Fig. 4 was preferred, as the top and bottom edges of the glass windows no longer obstruct visualisation of the parts of the flame closest to the chamber floor and ceiling.

The effective width of the channel can be altered by inserting a new glass spacer, of length equal to the channel length, at the desired position in the channel and parallel to the windowed edges. In this way, the channel was often operated at a width of 20 mm, which resulted in a narrow, uniform flame front that was well suited to direct photography from the side.

Fuel ignition was carried out using several igniters simultaneously along the fuel edge to generate a linear flame just upstream of the channel exhaust. A Canon A640 digital camera and a Sony Handycam captured photographic stills and video.

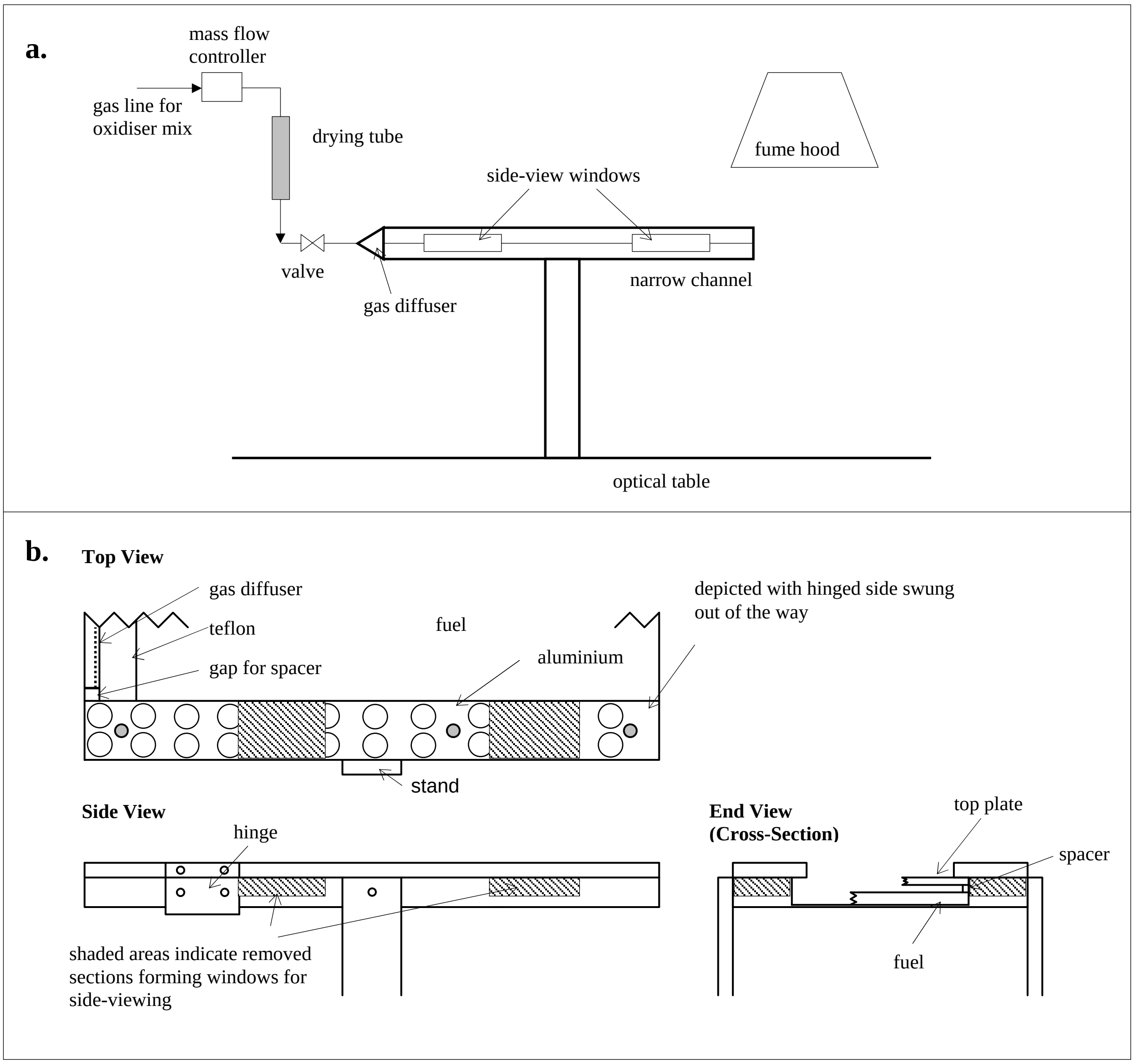

FIGURE 3. Experimental setup (a) Schematic of gas flow (b) Detail of narrow channel apparatus

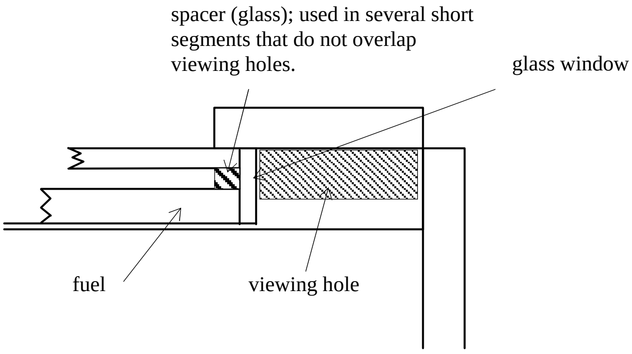

FIGURE 4. End view detail of modified NCA

A 2 mW He-Ne laser was chosen as the schlieren light source due to its several advantages; namely, it has high intensity over a broad beam area, and the model used incorporated internal components to spatially filter, expand and collimate the beam. The laser was mounted on a vibration-damping post, in a housing with a fine pan and tilt adjustment mechanism. All optical components were attached to an optical bench.

Lenses were chosen for focussing instead of mirrors. The advantages afforded by the compact lens setup were found to outweigh the negligible losses in image quality due to the beam traversing the lens and exposing any flaws in the material. The knife-edge was mounted using a two-axis screw-gauge travelling system to allow extremely fine adjustments in position. The image projected onto the screen was recorded by a Sony Handycam video recorder.

RESULTS AND DISCUSSION

The flame was studied using direct photography for both floor and ceiling spread with channel heights of 6.5 mm and 4 mm, and with high and low gas inlet rates of 4.5 cm/s and 16.5 cm/s respectively. Schlieren images were obtained for 6.5-mm channel only, at high flow rate. Most experiments were carried out using pure oxygen.

When imaging the flame in the NCA at low flow rates, difficulty was encountered in establishing a straight flame front with a uniform cross-section, important when viewing the flame from the side. Under low-oxygen conditions the flame front begins to become sinusoidal or ‘notched’ before ultimately starting to form fingers[15]. Fig. 5 shows a typical example. This problem could be overcome by narrowing the channel to 20 mm when using photographic imaging, and using an inlet gas rate of more than 4 cm/s. For schlieren imaging, the full 112 mm of the channel width was used to ensure a greater cumulative deviation of the laser beam and hence a greater contrast in the schlieren image.

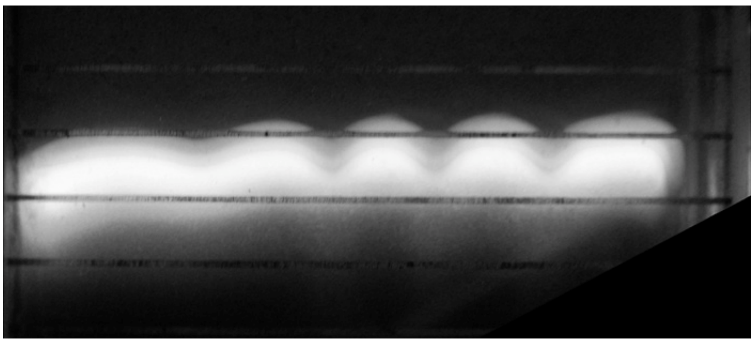

FIGURE 5. Top view of flame front with the onset of fingering. Direction of propagation is towards the top of the page. Reference lines are spaced by 10 mm.

Photographic Images of Flame Profile

Direct photography allowed the flame profile to be studied qualitatively. Fig. 6a shows the flame profile for floor and ceiling spread in a 6.5-mm channel at gas inlet rate of 16.5 cm/s of O_2. The main body of the flame is blue, and closer to the fuel is a bright orange zone of partially-combusted fuel vapour. The floor and ceiling flames are qualitatively similar with approximately the same flame length. The rate of ceiling flame spread was measured at 0.41 ± 0.04 cm/s, and the floor spread rate at 0.45 ± 0.04 cm/s.

Fig. 6a shows the presence of a fine, blue flame front extending 4 mm ahead of the main ceiling-spread flame zone. Fig. 7 shows an example of the phenomenon captured for floor spread using a full-width chamber to give a brighter (but less well-defined) flame zone image; the leading flame tongue is clearly visible and extends 10 mm in front of the main combustion zone. It is has not been determined whether this feature extends across the full front of the flame or whether it is only present at the chamber boundaries. It is hypothesised that it is a result of solid-phase conduction ahead of the main flame front.

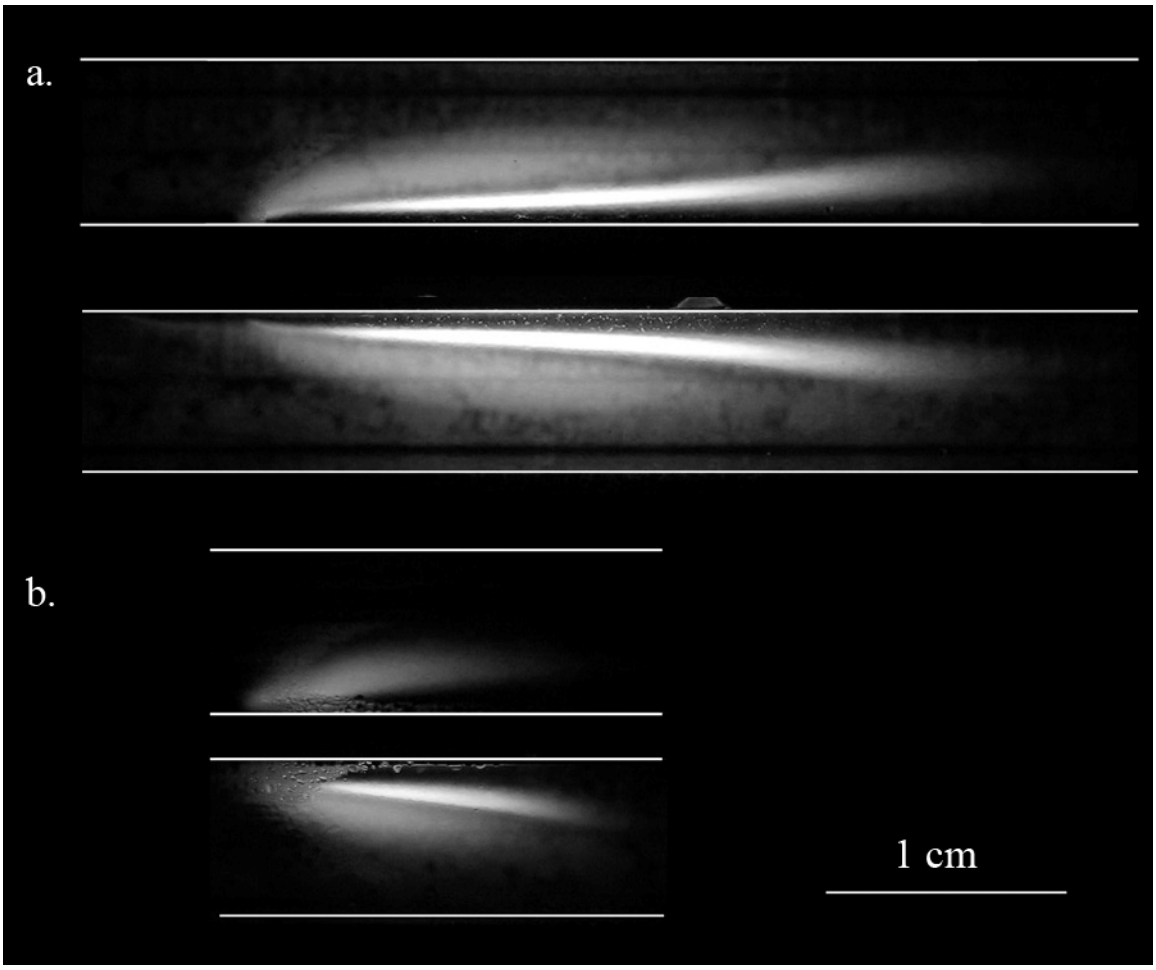

FIGURE 6. Photographic images of floor and ceiling spread towards the left, in 6.5 × 20 mm channel with 100% O_2 at (a) 16.5 cm/s, exposure times 1/125 s; (b) 4.5 cm/s, exposure times 1/40 and 1/30 s. The tip of the ceiling flame in (b) is partially obscured by condensation on the glass.

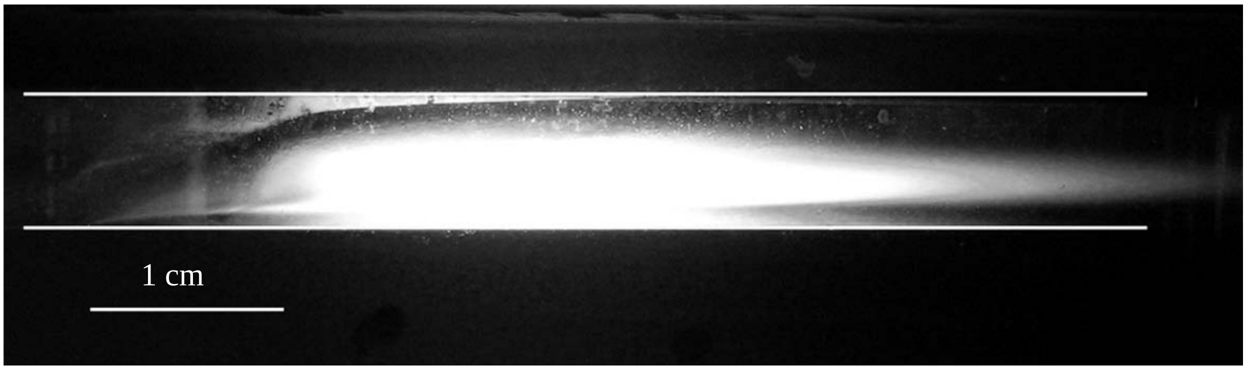

FIGURE 7. Photographic image of floor spread towards the left, in 6.5 × 112 mm channel with 100% O_2 at 16.5 cm/s; exposure time 1/125 s.

Effect of reducing oxygen flow rate. When the oxygen inlet rate was reduced from 16.5 to 4.5 cm/s, the flame lengths and propagation rates decreased, and the floor and ceiling flames became qualitatively different. Fig. 6b shows a comparative image. The ceiling flame exhibited less-complete combustion than its floor equivalent, which was a uniform blue. The ceiling flame propagated at 0.25 ± 0.02 cm/s, which was 71% of the floor-spread flame speed of 0.35 ± 0.04 cm/s. In addition, visual inspection of fuel after burning also shows a black, sooty residue left on the surface during ceiling-spread trials, which is not present after floor-spread trials. The less complete combustion for ceiling trials is possibly due to convection currents causing the vaporised fuel molecules to remain close to the fuel surface, leading to less thorough mixing of oxygen with fuel vapour near the surface and hence less heat transfer back to the solid fuel.

Effect of reducing channel height. Photographic images were obtained for flame spread in a channel of height 4 mm in both floor and ceiling configurations, for the same linear gas flow rates as used with the 6.5-mm channel. Fig. 8 shows to-scale pairs of photographs of floor and ceiling spread for high and low gas inlet rates respectively. The flame length has reduced compared to the 6 mm-channel flames.

The floor and ceiling flames were qualitatively similar. For high gas flow rate, the ceiling flame exhibited a slightly more prominent zone of yellow partially combusted fuel vapour. For low flow rate there was much less difference in structure between floor and ceiling modes than for the 6.5-mm channel. For both flow rates, the flame heights in the 4-mm channel are approximately the same as for tests using the 6.5-mm channel, but representing different percentages of the channel height.

Schlieren Images of Flame Profile

Schlieren imaging was used to study flame under 4.1 cm/s of pure O_2 for the 6.5-mm channel. It allowed several extra features of the flame to be observed and measured. These included the gaseous and solid thermal lengths (the preheat zone) and the heat transfer in the solid fuel.

Fig. 9 shows a typical visual image of a flame, presented together with a schlieren image taken under the same experimental conditions for comparison. For clarity, a duplicate schlieren image is shown with interesting features identified. The markings visible on the fuel in the schlieren image are due to a pattern created when the fuel piece was cut.

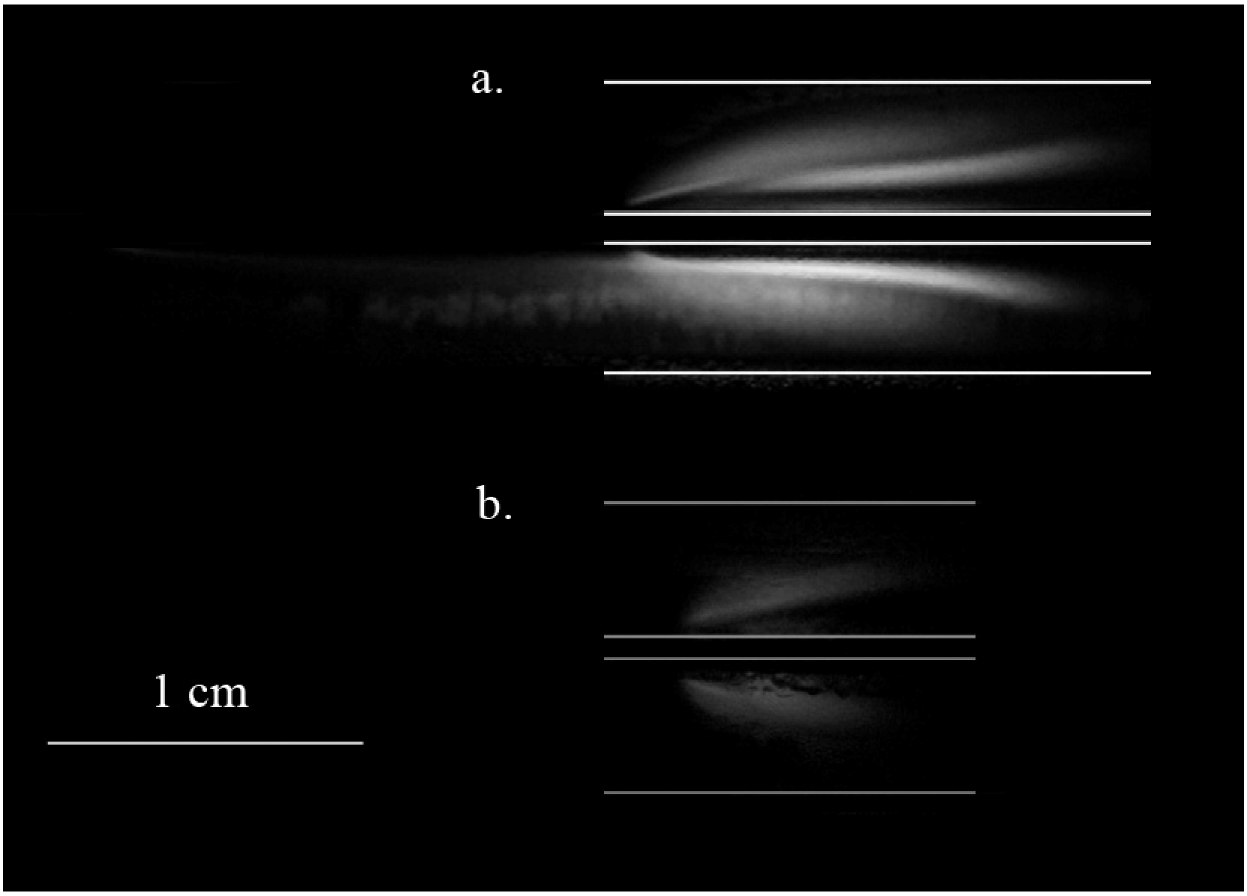

FIGURE 8. Photographic image of floor and ceiling spread towards the left, in 4 × 20 mm channel with 100% O_2 at (a) 16.5 cm/s, exposure times 1/250 and 1/160 s; (b) 4.5 cm/s, exposure times 1/125 s.

The combustion zone appears in the image as a bright area. Flaws in the upper and lower edges of the glass spacers obscure the top and bottom of the channel, blocking visualisation of the flame tip. The bright area ahead of the flame front represents the distance of forward heat transfer, or the gaseous thermal length. As the fuel heats it becomes dark under schlieren imaging; the boundaries of this dark region have been taken to approximate the limit of heat transfer in the fuel, and hence the solid thermal length is measurable and is annotated on Fig. 9. Over several trials with 100% O_2 at a flow rate of 4.1 cm/s, the gaseous thermal length was found to be 1.1 ± 0.1 cm, and the solid thermal length was found to be 0.8 ± 0.2 cm. The maximum depth to which the solid temperature changes can also be obtained from schlieren images, and was found to be 0.51 ± 0.05 cm.

Using the knife edge in a vertical orientation accentuated certain features. Fig. 10 shows how the gaseous thermal length is more easily visible, but information about combustion zone profile is lost.

Images similar to Figs. 9 and 10 were obtained for ceiling spread. In addition to the differences in flame shape, colour, length and propagation speed already observed, the schlieren images identified differences between floor and ceiling spread for thermal lengths and the depth of heat transfer into the solid. This indicates that at the test height, chamber conditions for combustion do not mimic microgravity.

Notably for ceiling spread, the solid and gaseous thermal length are no longer approximately equal to each other, which suggests a different dominant heat transfer method than for floor flow. The solid thermal length was measured at 0.25 ± 0.2 cm; these values are significantly lower than the 0.8 ± 0.2

cm for floor spread. The depth of heat transfer into the solid was 0.31 ± 0.04 cm, compared to 0.51 cm for floor spread. The gaseous thermal length was found to be 1.1 ± 0.2 cm, which shows agreement with the floor spread value of 1.1 ± 0.1 cm. These values indicate that the gas-phase conduction is unaltered by inverting the channel despite the lack of complete combustion, and suggest that the major source of difference is heat transfer through the fuel, probably altered by fuel-vapour convection.

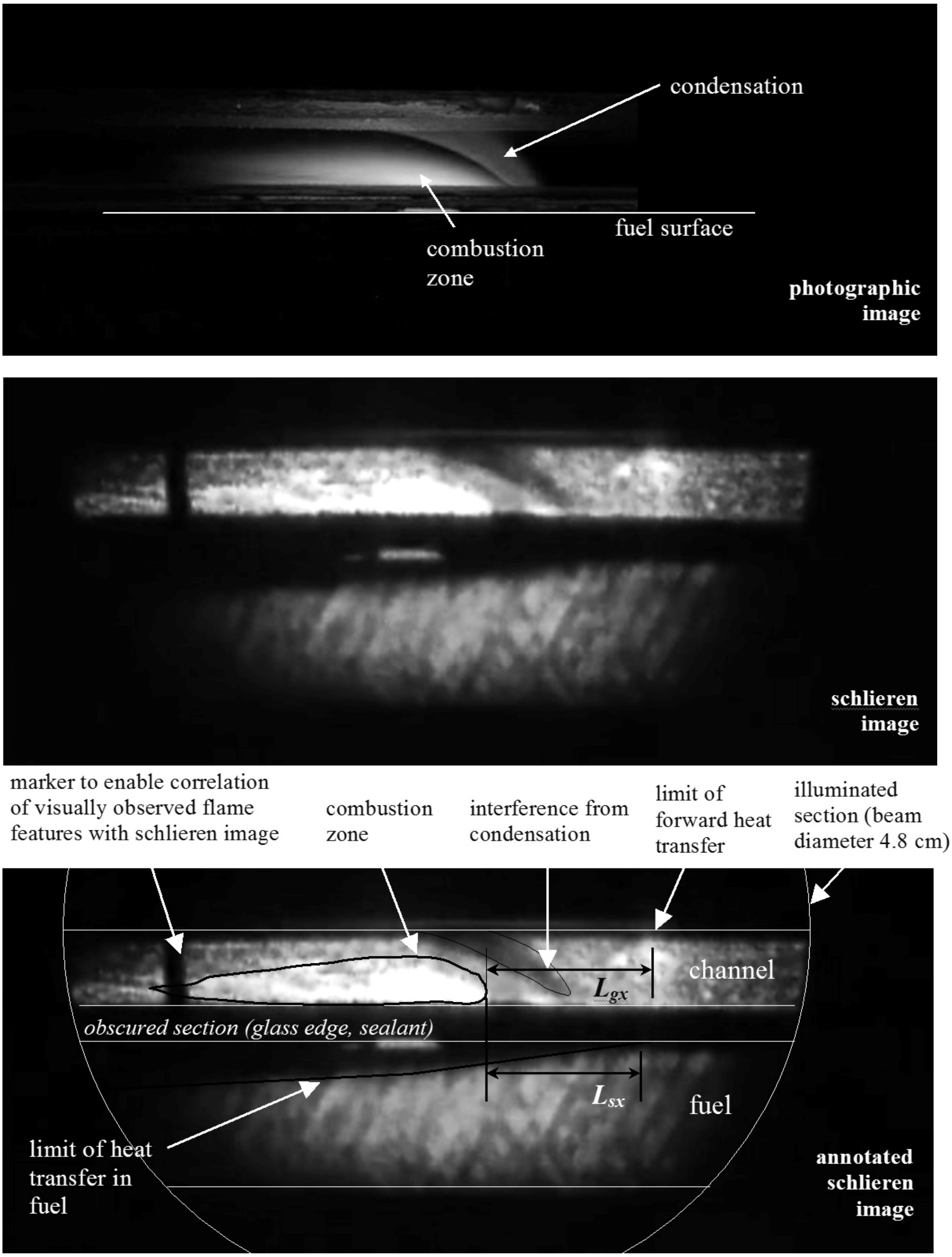

FIGURE 9. Schlieren images of floor-spread flame in NCA, propagating L to R; top: direct photograph; middle: schlieren image; bottom: annotated image (Horizontal knife edge; 100% O_2 @ 4.1 cm/s)

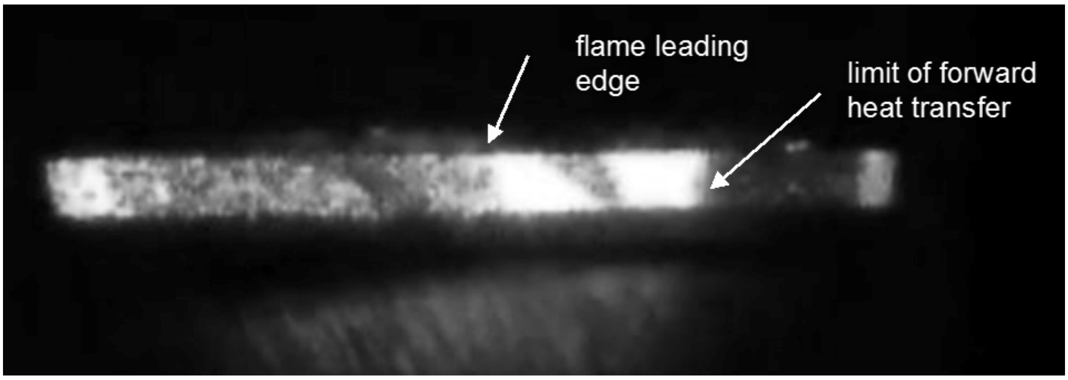

FIGURE 10. Schlieren image demonstrating well-defined gaseous thermal length, obtained by using vertical knife-edge. (0° orientation, vertical knife edge, 100% O_2 @ 3.7 cm/s)

CONCLUSIONS

Photographic and schlieren images were shown to have potential as a technique for investigating thermal properties of a flame in a narrow channel apparatus. The flame profile was photographed under a range of operating conditions; higher gas inlet rates and smaller channel heights were found to result in a better approximation to microgravity for the apparatus. This was found by comparing the qualitative profile of floor and ceiling spread flames for a given set of operating conditions.

In the 6.5-mm channel the solid and gaseous thermal lengths were able to be measured from schlieren images. The solid thermal lengths were shown to be 0.8 ± 0.2 cm for floor spread and 0.25 ± 0.2 cm for ceiling spread; both chamber orientations resulted in gaseous thermal lengths within 1.1 ± 0.2 cm. It is believed that reduced migration of vapourised fuel particles away from the fuel surface causes partially incomplete combustion in ceiling spread, helping to explain the differences in observed quantities between the two channel orientations. These differences were reduced when the experiment was repeated in a 4-mm channel, which is therefore more successful in approximating a microgravity environment for combustion.

The flame length increased with higher oxidiser flow rate and larger channel height, in agreement with equation [2]. However, at a channel height of 6 mm the floor and ceiling flames were different shapes and lengths, indicating the need for a gravity-related term in the expression.

The onset of fingering at low oxygen concentration and flow rate limited the range of flame conditions that could be tested. Visual obstruction also occurred from condensation on the viewing windows, and from the edges of the glass viewing panels used for the schlieren setup.

ACKNOWLEDGEMENTS

The authors thank the Australian Research Council for funding the present work.

REFERENCES

1. Melikhov, A.S., Potyakin, V.I., Pyzhov, A.M. and Ivanov, B.A., "About Limited Regimes of Polymer Burning in Absence of Natural Convection", Fizika Goreniya I Vzryva (Phys. Combust. Explos.), 4, 27-30, 1983 - In Russian.
2. Delichatsios, M.A., Wang, H., Kennedy, E.M., Moghtaderi, B. and Dlugogorski, B.Z., "Opposed Flame Spread in Narrow Channel Apparatus to Assist in Suppression Studies", 8th International Symposium on Fire Safety Science, 481-492, 2005.

3. Olson, S.L., “Fuel Thickness Effects on Flame Spread and Extinction Limits in Low Gravity As Compared to Normal Gravity”, Fall Eastern States Section Meeting of the Combustion Institute, 101-1 – 101-4, 1991.
4. Bhattacharjee, S. and Altenkirch, R.A., “A Comparison of Theoretical and Experimental Results in Flame Spread Over Thin Condensed Fuels in a Quiescent, Microgravity Environment”, 24th Symposium (International) on Combustion, 1669-1676, 1992.
5. Bhattacharjee, S., Seminar presentation at http://eng.sdsu.edu/flame/scaling/meSeminar2001.ppt (accessed February 2006).
6. Chen, Y., Motevalli, V., Delichatsios, M.A. and Tatem, P.A., “Prediction of Horizontal Flame Spread using a Theoretical and Experimental Approach”, 27th Symposium (International) on Combustion, 2797, 1998.
7. Ito, A., Kudo, Y. and Oyama, H. “Propagation and Extinction Mechanisms of Opposed-Flow Flame Spread over PMMA for Different Sample Orientations”, Combust. Flame 142, 428-437, 2005.
8. Kudo, Y., Itakura, M., Fujita, Y. and Ito, A., “Flame Spread and Extinction over Thermally Thick PMMA in Low Oxygen Concentration Flow”, 8th International Symposium on Fire Safety Science, 457-468, 2005.
9. Urbas, J. and Parker, W.J., “Surface Temperature Measurement in a Fire Environment Using an Infrared Pyrometer”, 8th International Symposium on Fire Safety Science, 1401-1412, 2005.
10. Ferkul, P., Sacksteder, K.R., Greenberg, P.S., Dietrich, D.L., Ross, H.D., T’ien, J.S., Altenkirch, R.A., Tang, L., Bundy, M. and Delichatsios, M., “Combustion Experiments on the Mir Space Station”, 37th Aerospace Sciences Meeting, American Institute of Aeronautics and Astronautics, 1999.
11. Hicks, J., “Flame Spread across a Solid Fuel in a Narrow Channel”, University of Newcastle Chemical Engineering Honours Thesis, 2004.
12. Ibarreta, A.F. and Sung C.-J., “Flame Temperature and Location Measurements of Sooting Premixed Bunsen Flames by Rainbow Schlieren Deflectometry”, Applied Optics 44:17, 3565, 2005.
13. Feikema, D.A., “Quantitative Rainbow Schlieren Deflectometry as a Temperature Diagnostic for Spherical Flames”, 42nd Aerospace Sciences Meeting & Exhibit, 2004.
14. Greenberg, P.S., Klimek, R.B., Buchele, D.R., “Quantitative Rainbow Schlieren Deflectometry”, Applied Optics, 34:19 3810, 1995.
15. Zik, O., Olami, Z. and Moses, E., “Fingering Instability in Combustion”, Phys. Rev. Lett. 81, 3868-3871, 1998.